Med Sci Monit, 2001; 7(1): 153-163

# Towards MRI guided surgical manipulator

**Kiyoyuki Chinzei[1], Karol Miller[2]**

[1] Biomechanics Division, Mechanical Engineering Laboratory, MITI, Tsukuba, Ibaraki, Japan
[2] Department of Mechanical and Materials Engineering, The University of Western Australia Crawley/Perth, Australia

**key words:** magnetic resonance compatibility, surgical robot, brain, mechanical properties, finite element method

## SUMMARY

***Background:*** *The advantages of surgical robots and manipulators are well recognized in the clinical and technical community. Precision, accuracy and the potential for telesurgery are the prime motivations in applying advanced robot technology in surgery. In this paper critical interactions between Magnetic Resonance Imaging equipment and mechatronic devices are discussed and a novel Magnetic Resonance compatible surgical robot is described.*
***Material and Methods:*** *Experimental results of the effects from several passive (metallic materials) and active (ultrasound motors) mechanical elements are demonstrated. The design pronciples for Magnetic Resonance compatible robots are established and the compatibility of the proposed robot is assessed by comparing images taken with and without the robot's presence within Signa SP/I GE Medical Systems scanner.*
***Results:*** *The results showed that, in principle, it is possible to construct precision mechatronic devices intended to operate inside MR scanner. Use of such a device will not cause image shift or significant degradation of signal-to-noise-ratio. An MR compatible surgical assist robot was designed and constructed. The robot is not affected by the presence of strong magnetic fields and is able to manoeuvre during imaging without compromising the quality of images. A novel image-guided robot control scheme was proposed. As a part of the control scheme, biomechanics-based organ deformation model was constructed and validated by in-vivo experiment. It has been recognised that for robust control of an image guided surgical robot the precise knowledge of the mechanical properties of soft organs operated on must be known. As an illustration, results in mathematical modelling and computer simulation of brain deformation are given.*
***Conclusion:*** *The novel MR compatible robot was designed to position and direct an axisymmetric tool, such as a laser pointer or a biopsy catheter. New Robot control system based on the prediction of soft organ deformation was proposed*

## BACKGROUND

The advantages of surgical robots and manipulators are well recognized in the clinical and technical community. Precision, accuracy, and the potential for telesurgery are the prime motivations in applying advanced robot technology in surgery [1–4]. Surgical robots require trajectory planning, which, in practice, relies upon preoperative images. If the target organ is deformable the trajectory needs to be updated according to the magnitude of the deformation. Here, image-guided surgery is a natural solution.

Magnetic resonance imaging (MRI) provides excellent soft tissue discrimination and a well-defined 3D coordinate reference system. An intra-operative MR scanner (Signa SP/i, GE Medical Systems,

**Sources of support: Japanese Agency of Industrial Science and Technology, Australian Research Council**

**Received:** 2000.11.20
**Accepted:** 2000.12.20

**Correspondence address:** Karol Miller, Department of Mechanical and Materials Engineering, The University of Western Australia
35 Stirling Highway, Crawley/Perth WA 6009, Australia, e-mail: kmiller@mech.uwa.edu.au

Milwaukee, WI, 0.5 Tesla) has been specifically designed to bring the power of MRI to the operating theatre. It has a pair of parallel facing donut-shaped magnets, with an air gap of 560 mm. Two surgeons can stand in the gap to access the patient. In the six years to February 2000, Brigham and Women's Hospital (Boston, MA), our collaborator, had recorded more than 500 cases using the intra-operative MR scanner [5–7].

In this paper, we demonstrate a unique configuration of a novel MR-compatible robotic system for use in MR guided surgery. The goal of our robot assist system is to enhance the surgeon's performance by accurate mechanics and numerical control, not to eject him or her from the surgical field. Therefore, the system must coexist and cooperate with the surgeon. Minimal-invasiveness is an obvious requirement. The system will actively navigate a small tool, such as a catheter needle, with 'pin-point' accuracy, under intra-operative MR guidance. Intra-operative images will serve as the source of trajectory revision. The robot can perform the insertion, however, our current plan reserves this task for a surgeon owing to ethical and legal considerations.

The environment of intra-operative MR scanner creates two requirements for the surgical robot design, in addition to the standard requirements such as safety and sterilization issues.

1) Kinematic structure (layout): The robot must coexist with a surgeon. However, when the patient is prepared and surgeons take their place, the available space for the robot is limited, particularly around the patient.

2) Magnetic Resonance compatibility: To enable real-time tracking of the target position, the robot should be able to manoeuvre, even during imaging. The robot motion should not have any adverse effect on the imaging, and it should not be affected by the imaging process. This requires that the robot be made from paramagnetic materials. In addition, the robot should be MR-safe. The MR safety of the robot requires that the machine should not unintentionally move as a result of magnetic attraction and adverse electromagnetic side effects (i.e. leakage of, and heating by, eddy currents and radio frequency (RF) pulses) should not occur.

The requirement of MR compatibility created major difficulties for device developers, in particular, for mechatronic designers who build robots. Standard mechanical parts cannot be used in MR environment because they usually contain ferromagnetic components. However, experimental and theoretical studies gradually established the design criteria to build MR compatible machines. Shellock intensively studied this subject and issued a guidebook of the compatibility for many medical devices [8]. Schenck defined MR compatibility and classified numerous materials [9]. GE Medical Systems disclosed their guidelines for the design of MR compatible devices intended for their intra-operative scanner [10]. It provides comprehensive and descriptive information about how developers should test the compatibility of their products. Hynynen developed MR guided focused ultrasound system [11]. It was actuated by ultrasonic (piezoelectric) motors. Masamune developed a surgical manipulator that could reside and work in the MR environment, not during imaging, though [12].

This paper will illustrate the criteria to design mechatronic devices to be MR compatible, assuming their use with open configuration scanners. Possible interactions between the mechatronic devices and the MR imaging equipment are discussed. The effects caused by several metal samples and mechanical parts in the intra-operative MR scanner are demonstrated. Based on these basic results an MR compatible surgical robot is proposed and the prototype described.

For the confident control of a surgical robot the properties of organs, on which it operates, must be known and the deformation of the organ caused by the robot movement must be predictable beforehand. As an illustration we present a computational model forecasting deformation of the brain under surgical load.

## MAGNETIC RESONANCE COMPATIBILITY OF MECHATRONIC DEVICES

In this section we review the definition of MR compatibility and discuss possible interactions between a mechatronic device and MRI. Then, we derive design criteria of mechatronic devices to be MR compatible. Some crucial devices were experimentally evaluated [13].

The most descriptive and practical definition of MR compatibility is found in [10]. It describes the experimental protocols to evaluate compatibility. General Electric [10] defines the following MR compatibility conditions of a foreign device:

— it is MR safe,

— its use in the MR environment does not affect imaging quality,

— it operates as designed in the MR environment.

In addition, location and timing zones, where MR compatibility with respect to each zone should be stated are defined. The proposed zones are as followings:

— Zone 1 device may remain in the image's region of interest and in contact with the patient during the surgical procedure and imaging.

— Zone 2 device may remain in the imaging volume and in contact with the patient during the surgical procedure and imaging, but the device is not in the region of interest.

— Zone 3 device is used within the imaging volume, but removed during imaging or when not in use.

— Zone 4 device can be used in the magnet room during the surgical procedure if it is kept a distance of more than ~1m from the magnet centre or outside the ~200Gauss line.

**Possible Interactions**

Various phenomena that can occur when a mechatronic device is placed adjacent to MRI scanner and is driven during imaging are listed below:

— Effect 1: Magnetic field attracts mechanical devices. The strong static magnetic field can attract ferrous parts in the passive and active devices. This may result in unexpected behaviour. For example, standard springs often do not function as expected inside Zone 3.

— Effect 2: Radio frequency (RF) pulse induces false signals in sensors. High-impedance sensors can induce the RF (radio frequency) pulse depending on the distance from and directivity of the RF coil. It is not easy to eliminate such induced signals.

— Effect 3: Foreign objects distort magnetic field. The effect of ferromagnetic objects in Zone 1 and 2 on the homogeneity of the magnetic field is obvious. Even a paramagnetic object can have some effect if it is conductive, due to the eddy current in Zones 1 and 2. Most of standard mechatronic devices are magnetically strongly incompatible.

— Effect 4: Foreign objects reduce performance of RF probe. The RF probe is a receiver antenna and is tuned to the resonance frequency. Foreign objects that are dielectric or conductive, and are adjacent to the probe, typically in Zones 1 to 2, can alter properties of the antenna.

— Effect 5: Wiring introduces noises. MR magnet room is an RF shield room. It cuts off electric noise from the outside and vice versa. A wire passing from outside to the magnet room can act as an antenna radiating electric noise. It can happen regardless of the distance from the scanner, significantly affecting the image quality, in particular, signal-to-noise-ratio (SNR).

— Effect 6: Foreign resonant objects affect gain controller. The gain controller of the signal receiver can be mistuned in the presence of a large source of resonance signal in Zone 1. This can occur when the imaging object is small in volume and a hydraulic or water driven actuator is in Zone 1.

**Design criteria**

*Structural element*

Many non-ferrous metals, ceramics, plastics, and composite materials are non-magnetic. Austenitic stainless steels (300~series) are neither ferromagnetic, nor paramagnetic. Their magnetic susceptibility ranges from $10^{-1}$ to $10^{-3}$. Titanium and aluminium are well known as MR compatible, but they are not ideally paramagnetic, hence they require some compromise if they were to be used in Zones 1 and 2. Other materials are often too soft except ceramics, which are too hard and brittle.

*Passive mechanical devices*

Gears, wire drives, cams, bearings, ball screws, linear guides, etc. are in this group. A variety of plastic parts is available. Unfortunately, due to their poor rigidity they cannot be used in more demanding applications. Ceramic devices are expensive, often heavy and cannot replace thin metallic parts. However, they are very hard and rigid. Ceramic bearings are widely available. The preferable choice seems to be paramagnetic metals, as will be described later.

**Table 1.** Hardness and magnetic susceptibility of typical metals.

| | Hardness (HB) | $\chi$ (x $10^{-6}$) |
|---|---|---|
| Be-Cu | 300-380 | 4 |
| YHD50 | 420 | 1900 |
| SUS440C | 580 | 109 |
| SUS316 | < 187 | 9000 |
| Al | < 150 | 20.7 |
| Ti | 100 | 182 |

Values from unpublished measurements by NSK Ltd. (Tokyo, Japan).

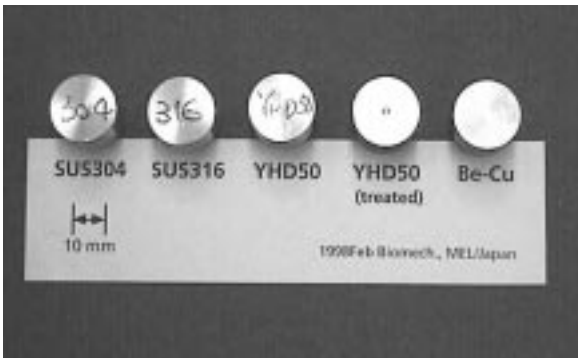


**Figure 1.** Sample chips. From left, stainless steel type 304, type 316, YHD50, surface treated YHD50, and Be-Cu.

*Active mechanical devices*

Actuators, clutches, and brakes fall into this category. Majority of these are electromagnetic and practically impossible to use inside Zone 3. Ultrasonic (piezoelectric) motor can serve as a substitute for electromagnetic motor [14,15]. It has been difficult to find good alternatives to electromagnetic clutches and brakes.

*Sensors*

Most of modern sensors are electric. They can emit noise and can receive false signals from the RF pulse.

*Electromagnetic interference (EMI)*

EMI can occur even if the electric device is placed in Zone 4. To minimize EMI, the following techniques must be considered:

— Wires and circuits should be properly shielded, never use the shield as the current path,
— Cables of appropriate size and impedance should be used,
— Twisted pair cables are recommended,
— Shield should be properly grounded. Large ground loop should be avoided,
— Switching regulators, AC-DC converters, etc. should be avoided,
— Opto-isolation and inline noise filters should be considered.

**Magnetic resonance compatibility of hard paramagnetic metals**

*Metal Chips in Zone 1*

Passive mechanical devices require precise dimensions as well as smooth and hard surfaces. There are several candidates for this purpose: three austenitic stainless steels (type 304, 316, YHD50) and a beryllium-copper (BeA-25-HT; abbreviated as Be-Cu). YHD50 is a non-standardized new stainless steel (Hitachi Metals Ltd, Tokyo, Japan). Table 1 lists surface hardness and magnetic susceptibility of typical metals.

In order to assess MR compatibility of these materials it was necessary to experimentally evaluate their influence on image quality. We examined these metals in Zone 1.

**Material and methods:** Five cylindrical samples (height – 22mm, diameter – 20mm, stainless steels type 304, type 316, YHD50, YHD50 with surface hardening treatment, and Be-Cu) were prepared, Figure 1. Each of these was put in the NiCl2 solution and 2D scans that axially intersected the samples were acquired. Every metallic object produced a void (dark) shadow that had no resonance signal. The object also distorted the magnetic field around it: the larger the void the larger the distortion. We observed the size of the shadow.

**Results:** Beryllium-copper showed the smallest void, see Figure 2. YHD50 after surface treatment showed larger void, which meant degradation of paramagnetism.

*Ball Screws in Zones 2-3*

We also examined the effect of mechanical devices made from candidate metals.

**Material and Methods:** Two ball screws, Figure 3, were examined: one made of YHD50 and another of beryllium-copper. Images of a spherical phantom containing CuSO4 solution were observed. The changes in the image caused by altering the

**Table 2.** Signal to noise ratio (SNR) of images with ball screws.

| (distance from isocenter) | 240 | 330 | 520 (mm) |
|---|---|---|---|
| Be-Cu ball screw (aligned) | 55.6 | 55.6 | 55.6 |
| Be-Cu ball screw (perpendicular) | - | - | - |
| YHD50 ball screw (aligned) | 57.5 | 57.5 | 57.5 |
| YHD50 ball screw (perpendicular) | - | - | - |
| Control (no object) | | 59.1 | |

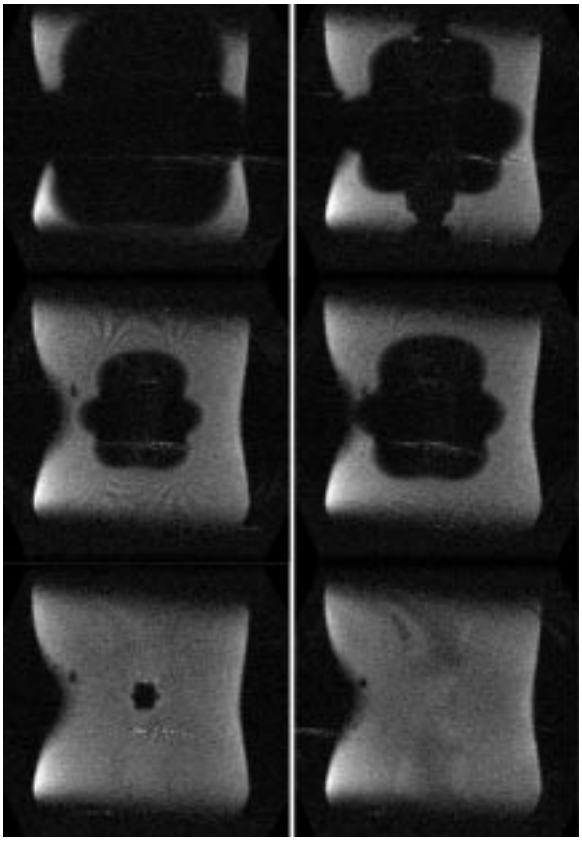

**Figure 2.** Effect of metallic samples on image quality. From left, stainless steel type 304, type 316, YHD50, surface treated YHD50, Be-Cu, and the control, respectively. Void is caused by the distortion of the magnetic field.

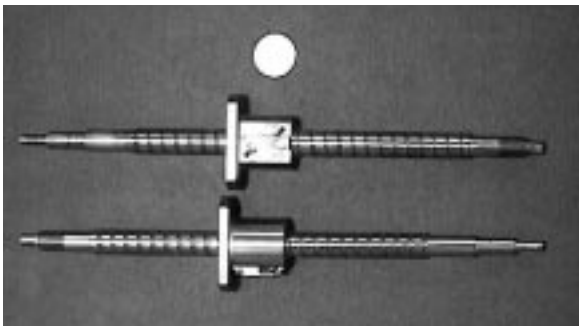

**Figure 3.** Be-Cu (upper), YHD50 (lower) ball screws.

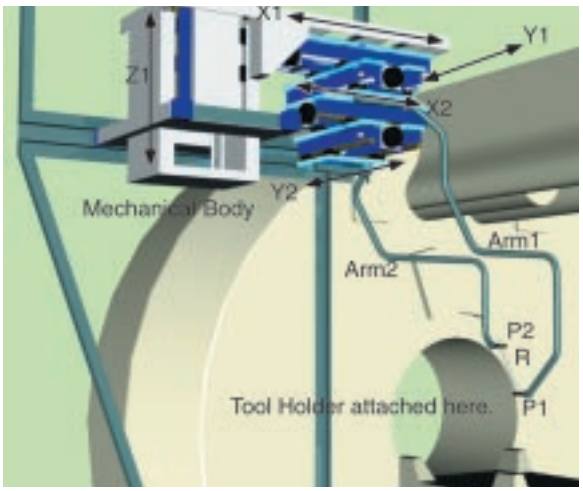


**Figure 4.** Robot axes layout. X1, Y1, Z1, X2 and Y2 are actuated.

**Table 3.** Signal to noise ratio (SNR) of images with ultrasonic motor driving during imaging.

| (distance from isocenter) | 240 | 330 | 520 (mm) |
|---|---|---|---|
| Motor ON 75 % of max speed | 54.4 | 64.0 | 55.5 |
| Motor OFF, unplugged from amplifier | 58.4 | 55.8 | 59.2 |
| Control (no object) | | 59.1 | |

distance between the screw and the centre of the imaging volume were compared.

**Results:** The obtained images looked identical. Image shift was not observed. Table 2 lists the signal-to-noise-ratio (SNR) values. The high SNR values correspond to high image quality. Significant loss of SNR was not observed.

### Magnetic resonance compatibility of active elements: ultrasonic motor (USM) in Zones 2-3

The operation of ultrasonic motors is not based on electromagnetic phenomena. However, the motors are driven by electric power. Therefore, the effect of possible electric noise should be evaluated.

**Material and Methods:** The influence of placing a rotating or stationary ultrasonic motor in the scan-

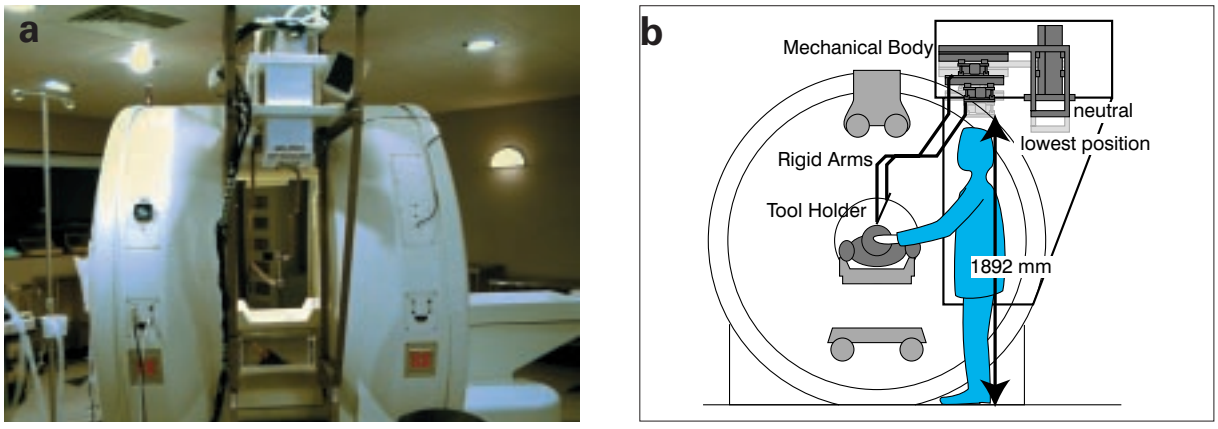


**Figure 5.** Constructed robot attached to the intra-operative MR scanner (a) and the profile of the workspace (b). The moving part does not obstruct the workspace of the surgeon.

**Table 4.** Observed inhomogeneity values. The smaller the value the greater the homogeneity.

| | Inhomogeneity (ppm) |
|---|---|
| Spherical phantom, without robot (baseline) | 0.45 |
| Spherical phantom, with moving robot | 0.53 |
| Spherical phantom, with an 'MR compatible' Mayfield stereotactic frame | 0.9 |
| Human volunteer | ca. 1.4 |

ner on the image quality was observed. The motor used was USM-60N1 (Shinsei Kogyo Corp, Tokyo, Japan). The effect was evaluated by the same methods as described in the previous section.

**Results:** There was neither image shift nor significant degradation of SNR values. This conclusion was valid for stationary as well as rotating motor; see Table 3.

## MAGNETIC RESONANCE COMPATIBLE ROBOT

The results of Section 2 have been applied in the design of the five-axis surgical manipulator [16], Figures 4 and 5.

### Configuration

Figure 4 shows a schematic configuration of the robot. The actuators and the end effector are spatially separated. The main body with all actuators is located above the surgeon's head. The end-effector is attached at the ends of two long, rigid arms. The robot has five degrees of freedom. Five degrees of freedom are sufficient to position and

**Figure 6.** Rigid arms and pivot joints. The arms can be divided into parts small enough to be autoclaved.

direct a catheter or a laser pointer because these instruments are axisymmetric.

### MR compatibility design and its evaluation

The five degree-of-freedom main body is composed of five linear motion tables. Each table unit has a ball screw and a pair of linear guides. These are made of either stainless steel (YHD50) or beryllium-copper. As shown in Section 2 both materials have low magnetic susceptibility and a hard surface that can be used as a point-touch mechanism. The ball screws and linear guides made from YHD50 were manufactured by NSK Ltd. (Tokyo, Japan), and those made from beryllium-copper were manufactured by Koyo Seiko Co, Ltd. (Osaka, Japan.) The ball-screw is supported by a pair of ball bearings made from silicon nitride (Si3N4) ceramics.

Non-magnetic (piezoelectric) ultrasonic motors, USR60-S3N, (Shinsei Kogyo Corp, Tokyo, Japan)

directly drive ball screws. Motor's maximum rotational torque is 0.5 Nm, and its holding torque is more than 0.7 Nm. A mechanical clutch was inserted between the motor and the ball screw to allow for manual motion.

All parts of the robot were made from paramagnetic materials. The rigid arms, the frame structure of the vertical axis, and the attachment of the robot to the scanner were made from a titanium alloy. For frames of the horizontal axes polycarbonate resin was used. Only titanium alloy or brass screws and bolts were used. A laser pointer, with minor modifications for MR compatibility, was attached. The arms can be divided into three pieces, Figure 6. The end pieces can fit in a typical autoclave tray, whose internal dimensions are approximately 450 x 80 x 200 mm.

The robot was equipped with linear optical encoders and optical limit detectors. We employed fibre optics to guide the signals to the optic sensors outside the magnet room. This technique was shown to be effective.

Cooperation between the robot control, MRI, and 3D position tracking was implemented by the object distribution server-client model [17] consisting of three modules: (1) a robot hardware module; (2) a Modular Robot Control (MRC) developed at Johns Hopkins University; and (3) Slicer3D modules (Image processing/surgical planning) [18]. For details see references [17,18].

The presence and motion of the robot can distort or shift the image by decreasing the homogeneity of the magnetic field. These can also affect the image signal-to-noise-ratio (SNR). To test that, a series of experiments was conducted.

**Material and Methods:** The images of a spherical phantom containing $CuSO_4$ solution were obtained while the robot manoeuvred inside the scanner. The robot repeated a simple Y2 axis motion, which was the most adjacent axis to the imaging region. The control data were obtained by the same phantom without the robot. The inhomogeneity of the magnetic field and the SNR were evaluated.

**Results:** The magnetic field inhomogeneity values are listed in Table 4. When the robot was in motion the inhomogeneity value of 0.53 was observed. This was better than that of a clinically used stereotactic frame or of the human body itself. Therefore, the robot effect on the homogeneity of the magnetic field was negligible.

The observed signal-to-noise ratio (SNR) loss was 1.6% to 1.8%. As an SNR loss up to 10% is acceptable, the observed SNR was in the negligible range. Figure 7 shows an image of the spherical phantom with, and without the robot.

These results indicated that the presence and the motion of the robot did not affect imaging. Also, we did not observe any unintended behaviour of the robot system that could be attributed to operation during imaging. The robot itself was not affect-

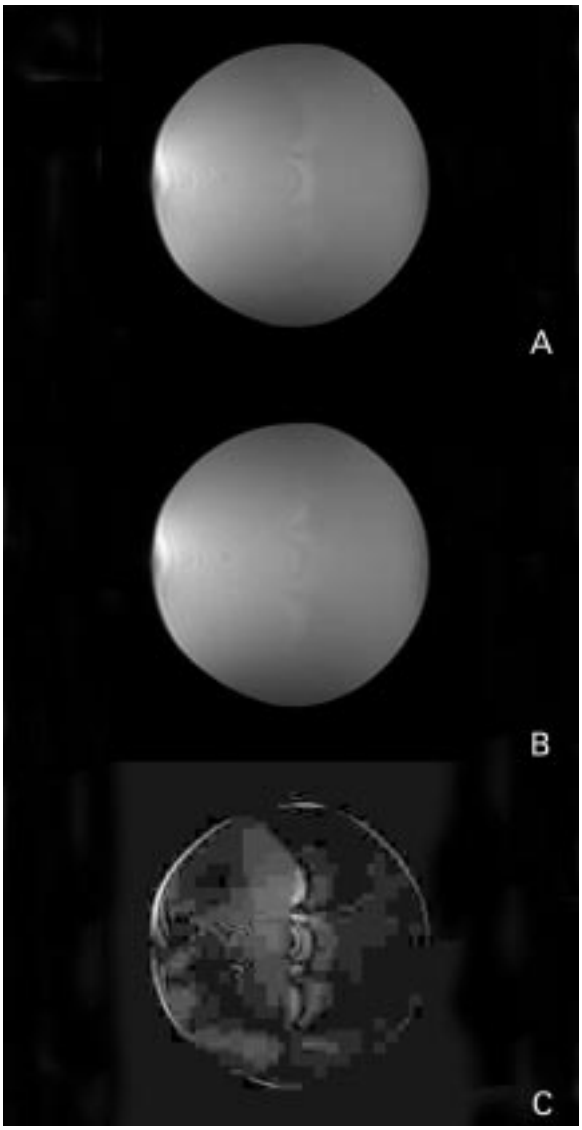


**Figure 7.** Images of the spherical phantom when the robot was not installed (a) and when one axis of the robot was in motion (b). The subtraction of these images showed no shift (c).

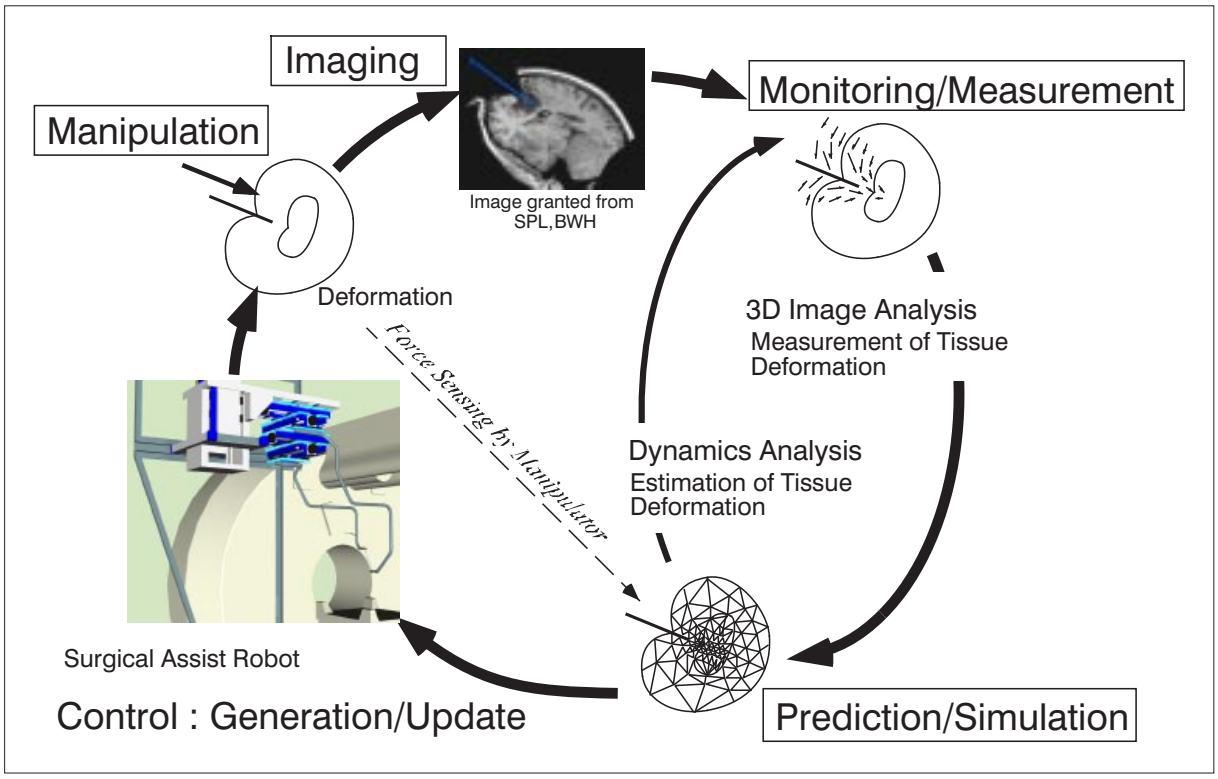


**Figure 8.** The concept of computer-based prediction part in the MRI guided robot control system

ed by the imaging process. We conclude that the robot proposed is MR compatible.

### Possible Applications

Intended first application of the presented robotic system is needle navigation in the brachytherapy of prostate cancer. This is a minimally invasive outpatient radiotherapy that delivers an internalised radioactive source to the tumour. A number of small iodine-125 radiation seeds are placed using catheters, under the guidance of MRI [19]. This procedure implants 50 to 120 seeds by 12 to 20 catheter insertions, according to a preoperative seeding plan. The seeding was previously performed using ultrasound or CT guidance. These methods could not adjust for any prostate motion, and could not delineate normal or abnormal structures in three dimensions. MR guidance offers greater spatial resolution and soft tissue discrimination.

Currently, a human operator manually inserts the catheter, so that the shadow of the catheter follows the planned trajectory on the display. It is a difficult task, requiring high level of skill. At the same time it presents itself as a good application for the robot.

## COMPUTER SIMULATION OF TISSUE DEFORMATION

In recent years, driven by developments in virtual reality techniques [20] and the emergence of automatic surgical tools and robots (e.g. [21]), new exciting area of research has emerged - computer simulation of surgical procedures. The prerequisite for such a simulation is an appropriate mathematical model of the tissue mechanical properties. This includes faithful representation of geometry, boundary and loading conditions as well as material properties of soft organs. Computer programs enabling accurate modelling of soft tissue deformation are needed in a surgical robot control system, where the prediction of deformation is needed [22,23].

The distinguishing feature of the mathematical model of the tissue intended for the simulation of surgery is the strain rate range (the loading speed range) considered – 0.01–1.0 $s^{-1}$ – orders of magnitude lower than that experienced in situations leading to injury. During loading resulting in such strain rates both non-linear stress-strain and stress-strain rate relations demonstrate their importance [24].


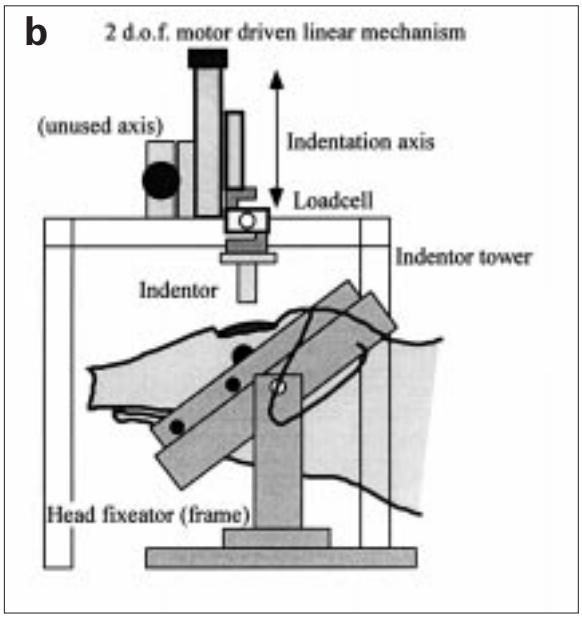


**Figure 9.** In-vivo indentation of swine brain – experiment configuration: a) general view; b) schematic of the set-up.

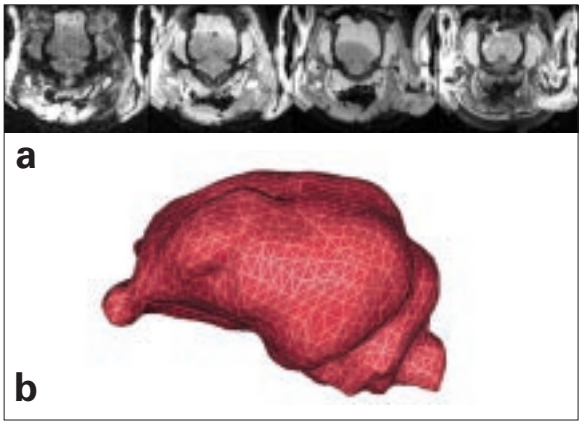


**Figure 10.** Examples of cross-section images of swine brain (a) and the shape of the brain after image segmentation (b)

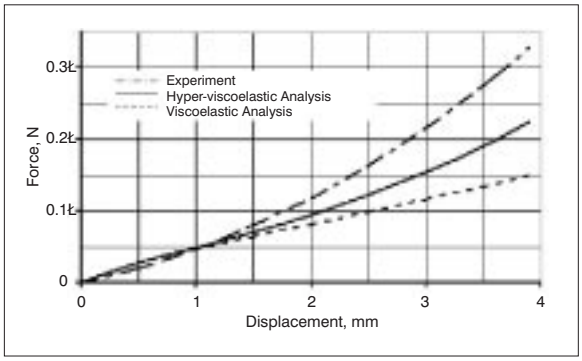


**Figure 11.** Force versus displacement relationship for 1mm/s indentation speed and 10mm indenter diameter: a) experiment; b) hyper-viscoelastic analysis results; c) linear, viscoelastic analysis results (for small strains the linear, viscoelastic model used had the same properties as the non-linear, hyper-viscoelastic model [24] instantaneous Young Modulus E=3240 Pa, Poisson's ratio n=0.499)

The schematic diagram of the application of computer simulation of organ deformation in MRI guided robot control system is given in Figure 8. During the operation the soft organ deforms significantly. This can be tracked by intra-operative MRI however, the time to produce and analyse 3D images is at least several seconds, likely more than tens of seconds. The proposed way of dealing with this delay is by using a computational model in the prediction part of the robot control system to calculate tissue deformation beforehand.

To validate mathematical models of brain deformation we conducted indentation of exposed swine brain tissue in-vivo. An approximately hundred days old Landrace swine under anaesthesia [25] was experimented on. The test was performed in the Surgeon Training Facility in Fujinomiya, Japan.

The brain was exposed by removing the skin, the skull and the dura. The exposed region, located on the front lobe, was of oval shape, approximately 25×20 mm. After exposing the brain, the head was fixated into a metallic frame with four sharp-end screws.

The main testing apparatus was a two-linear-degree-of freedom robot equipped with a strain-gauge load cell. The robot, fixed onto a rigid support, drove a cylindrical indenter of 10 mm diame-

ter. This allowed the flexibility of choosing the loading velocity and the depth of the indentation. Figure 9 shows the experimental setting.

Based on the estimates of the speed of surgeon's hands when conducting brain tissue separation (observed by the authors in Tokyo Women's Medical College Hospital), an indenter velocity of 1 mm/s was applied. The maximum depth of penetration of 3. 9 mm was set. The choice of the depth was based on our vast experience with swine brain tissue. We expected that the deeper indentation might inadvertently damage the brain and consequently kill the animal.

Theoretical analysis of the experiment required appropriate mathematical model of the experimental setting. Finite Element Method was used [26]. To develop finite element mesh precise knowledge of the sacrificed swine's geometry was needed. This was achieved by obtaining sectional magnetic resonance images of the swine's head and segmenting the image, see Figure 10. The details of the modelling procedure are given in [25]. Figure 11 shows a measured force (with heartbeat and respiration filtered out) versus time curve together with mathematical calculations using finite element method. The forces predicted by our model are about 31% lower than the measured ones. Taking into account the large variability inherent to biological materials, and the apparent stiffening of the tissue due to the tethering effect of a large number of blood vessels in the brain, the agreement, in our opinion, is good. The constitutive model used in this study is linear in parameters describing instantaneous response of the material [27]. Therefore, the increase of these parameters by 31% will result in almost perfect reproduction of the experimental force-displacement curve.

## CONCLUSIONS

The definition of MR compatibility was reviewed and the criteria to design mechatronic devices to be MR compatible were proposed. Low susceptibility / high hardness stainless steel YHD50 and beryllium-copper (Be-Cu) as well as other standard stainless steels (type 304 and type 316) were examined in Zone 1 of an intra-operative MR scanner. Be-Cu was proven to have the best performance in comparison to other materials, followed by YHD50. Ball screws made of these metals and an ultrasonic motor placed separately in Zones 2–3 did not cause significant loss of signal-to-noise-ratio nor any image shift.

Based on these results the robot was designed and the prototype constructed. The robot showed excellent Magnetic Resonance compatibility. Its motion did not have any adverse effect on the imaging and the robot itself was not affected by the imaging process.

Computational model for soft organ deformation was developed. Based on the in-vivo experimental results and computations the procedure of applying surgical simulation to neurosurgical planning can be suggested. Magnetic resonance images of a patient's head can be used to construct the mesh. Delicate indentation of the brain can then serve as a tool to adjust material constants in the mathematical model, without altering the model structure. The resulting model can next be used with some degree of confidence. However, more research is needed, especially into the appropriate modelling of the interface between the brain and the skull (boundary conditions). This direction of research, in the authors' opinion, is at least equally important to the investigation of the mechanical properties of brain internal structures.

Modern medicine has rich sources of information regarding the state of health of a patient. High quality three-dimensional images (e.g. MRI) transfer the real world (patient) into the virtual world. We have developed computer models for virtual manipulation for surgical planning. In contrast, the transfer from the virtual to the real world (i.e, the operating theatre) has been mostly limited to visual assistance. Here, the flow of online information is unidirectional and incomplete. Surgical robots will provide the means of physical assistance and create a bi-directional flow of online information. The impact of the combination of the intra-operative MRI, and the MR compatible robot, will be even greater, because it will bring the possibility of near real-time processing of the virtual and real worlds in a bi-directional manner.

**Acknowledgements**

The financial assistance of Agency of Industrial Science and Technology, Japan, and Australian Research Council is gratefully acknowledged.

## REFERENCES:


1. *Villotte N, Glauser D, Flury P et al: Conception of Stereotactic Instruments for the Neurosurgical Robot Minerva. Proc ieee icra, 1992; 1089-90*
2. *Taylor RH, Mitterlstadt BD, Paul HA et al: An Image-Directed Robotic System for Precise Orthopaedic Surgery. In Taylor RH, et al (eds): Computer-Integrated Surgery: Technology and Clinical Applications, MIT Press, 1995; 379-95*
3. *Sackier JM, Wang Y: Robotically Assisted Laparoscopic Surgery: from Concept to Development. In Taylor RH, et al (eds): Computer-Integrated Surgery: Technology and Clinical Applications, MIT Press, 1995; 577-80*
4. *Schenker PS, Das H, Ohm TR: A New Robot for High Dexterity Microsurgery. In Proc CVRMed95, Lecture Notes Computer Science, 905, Springer-Verlag, 1995; 115-22*
5. *Schenck JF, Jolesz FA, Roemer PB et al: Superconducting Open-Configuration MR Imaging System for Image-Guided Therapy. Radiology, 1995; 195(3): 805-14*
6. *Silverman SG, Collick BD, Figueira MR et al: Interactive MR-guided biopsy in an open-configuration MR imaging system. Radiology, 1995; 197: 175-81*
7. *Hata N, Morrison PR, Kettenbach J et al: Computer-assisted Intra-Operative Magnetic Resonance Imaging Monitoring of Interstitial Laser Therapy in the Brain: A Case Report. J Biomedical Optics, 1998; 3(3): 304-11*
8. *Shellock FG: Pocket Guide to MR Procedures and Metallic Objects: Update 1998. Lippincott-Raven publishers, Philadelphia 1998*
9. *Schenck JF: The role of magnetic susceptibility in magnetic resonance imaging: MRI magnetic compatibility of the first and second kinds. Med Phys, 1996; 23(6): 815-50*
10. *GE Medical Systems (eds): MR Safety and MR Compatibility: Test Guidelines for Signa SP. www.ge.com/medical/mr/iomri/safety.htm, 1997*
11. *Hynynen K, Darkazanli A, Unger E, Schenck JF: MRI-guided non-invasive ultrasound surgery. Med Phys, 1992; 20: 107-116*
12. *Masamune K, Kobayashi E, Masutani Y et al: Development of an MRI compatible Needle Insertion Manipulator for Stereotactic Neurosurgery. J Image Guided Surgery, 1995; 1: 242-8*
13. *Chinzei K, Kikinis R, Jolesz FA: MR Compatibility of Mechatronic Devices: Design Criteria. Proc MICCAI '99, Lecture Notes in Computer Science, 1999; 1679: 1020-31*
14. *Sashida T, Kenjo T: Introduction to Ultrasonic Motor (Chouonpa Motor Nyuumon; in Japanese). Sogo Denshi Shuppan, Tokyo, 1991*
15. *Crivii M, Jufer M: Piezoelectric ultrasonic motor - design and comparison. Proc Annual Symposium Incremental Motion Control Syst Devices, 1994; 23: 35-40*
16. *Chinzei K, Hata N, Jolesz FA, Kikinis R: MR Compatible Surgical Assist Robot: System Integration and Preliminary Feasibility Study. Proc MICCAI 2000, Pittsburgh PA, 2000; 921-930*
17. *Schorr O, Hata N, Bzostek A et al: Distributed Modular Computer-Integrated Surgical Robotic Systems: Architecture for Intelligent Object Distribution. Proc MICCAI 2000, Pittsburgh PA, 2000; 765-74*
18. *Gering D, Nabavi A, Kikinis R et al: An Integrated Visualization System for Surgical Planning and Guidance Using Image Fusion and Interventional Imaging. Proc. MICCAI '99, Lecture Notes in Computer Science, Springer-Verlag, Berlin, Heiderberg, New York, 1999; 1679: 809-19*
19. *D'Amico AV: Real-time magnetic resonance image-guided interstitial brachytherapy in the treatment of select patients with clinically localized prostate cancer. Int J Radiat Oncol Biol Phys, 1998; 42(3): 507-15*
20. *Burdea G: Force and Touch feedback for Virtual Reality. Wiley. New York, 1996*
21. *Brett PN, Fraser CA, Henningan M et al: Automatic Surgical Tools for Penetrating Flexible Tissues. IEEE Eng Med Biol, 1995; 264-270*
22. *Miller K, Chinzei K: Modeling of Soft Tissues, Mechanical Engineering Laboratory News, 1995; 12: 5-7 (in Japanese)*
23. *Miller K, Chinzei K: Modeling of Soft Tissues Deformation, Journal Computer Aided Surgery, Supl, Proc. of Second International Symposium on Computer Aided Surgery, Tokyo Women's Medical College, Shinjuku, Tokyo, 1995; 1: 62-63*
24. *Miller K, Chinzei K: Constitutive Modelling of Brain Tissue; Experiment and Theory. J. Biomech. 1997; 30 (11/12): 1115-112*
25. *Miller K, Chinzei K, Orssengo G, Bednarz P: Mechanical properties of brain tissue in-vivo; experiment and computer simulation, J. Biomech, 2000; 33/11: 1369-1376*
26. *Bathe K-J: FE Procedures in Engineering Analysis. Prentice Hall, USA, 1982.*
27. *Miller K: Constitutive Model of Brain Tissue Suitable for Finite Element Analysis of Surgical Procedures. J Biomech, 2000; 32: 531-537*

# Index Copernicus

## Global Scientific Information Systems for Scientists by Scientists

TM
INDEX COPERNICUS INTERNATIONAL

**www.IndexCopernicus.com**


- EVALUATION & BENCHMARKING
- PROFILED INFORMATION
- NETWORKING & COOPERATION
- VIRTUAL RESEARCH GROUPS
- GRANTS
- PATENTS
- CLINICAL TRIALS
- JOBS
- STRATEGIC & FINANCIAL DECISIONS

# Index Copernicus integrates

### IC Scientists

Effective search tool for collaborators worldwide. Provides easy global networking for scientists. C.V.'s and dossiers on selected scientists available. Increase your professional visibility.

### IC Virtual Research Groups [VRC]

Web-based complete research environment which enables researchers to work on one project from distant locations. VRG provides:

- customizable and individually self-tailored electronic research protocols and data capture tools,
- statistical analysis and report creation tools,
- profiled information on literature, publications, grants and patents related to the research project,
- administration tools.

### IC Journal Master List

Scientific literature database, including abstracts, full text, and journal ranking. Instructions for authors available from selected journals.

### IC Patents

Provides information on patent registration process, patent offices and other legal issues. Provides links to companies that may want to license or purchase a patent.

### IC Grant Awareness

Need grant assistance? Step-by-step information on how to apply for a grant. Provides a list of grant institutions and their requirements.

### IC Conferences

Effective search tool for worldwide medical conferences and local meetings.

### IC Lab & Clinical Trial Register

Provides list of on-going laboratory or clinical trials, including research summaries and calls for co-investigators.